https://doi.org/10.5194/hess-2022-246
Preprint. Discussion started: 7 July 2022

Hydrology and Earth System Sciences
Discussions
Open Access
EGU

Controls on leaf water hydrogen and oxygen isotopes: A local investigation across seasons and altitude

Jinzhao Liu[a, b*], Huawu Wu[c], Chong Jiang[a], Li Guo[d], Haiwei Zhang[e], Ying Zhao[f]

[a] State Key Laboratory of Loess and Quaternary Geology, Institute of Earth Environment, Chinese Academy of Sciences, Xi'an 710061, China

[b] National Observation and Research Station of Earth Critical Zone on the Loess Plateau of Shaanxi, Xi'an, 710061, China

[c] Key Laboratory of Watershed Geographic Sciences, Nanjing Institute of Geography and Limnology, Chinese Academy of Sciences, Nanjing 210008, China

[d] State Key Laboratory of Hydraulics and Mountain River Engineering & College of Water Resource and Hydropower, Sichuan University, 610065, Chengdu, China

[e] Institute of Global Environmental Change, Xi'an Jiaotong University, Xi'an, 710054, China

[f] College of resources and environmental engineering, Ludong University, 264025, Yantai, China

[*]Corresponding author's email: liujinzhao@ieecas.cn (J. Liu)

Abstract

The stable oxygen ($\delta^{18}O_{leaf}$) and hydrogen ($\delta^{2}H_{leaf}$) isotopes of leaf water act as a bridge that connects hydroclimate to plant-derived organic matter. However, it remains unclear

https://doi.org/10.5194/hess-2022-246
Preprint. Discussion started: 7 July 2022


Hydrology and Earth System Sciences
Discussions
Open Access
EGU

whether the source water (i.e., twig water, soil water, and precipitation) or meteorological parameters (i.e., temperature, relative humidity, and precipitation) are the dominant controls on $\delta^{18}O_{leaf}$ and $\delta^{2}H_{leaf}$. Here, we reported seasonal analysis of $\delta^{18}O_{leaf}$ and $\delta^{2}H_{leaf}$ together with isotopes from potential source waters and meteorological parameters along an elevation transect on the Chinese Loess Plateau. We found that $\delta^{2}H_{leaf}$ values were more closely correlated with source water isotopes than $\delta^{18}O_{leaf}$ values, whereas $\delta^{18}O_{leaf}$ and $\delta^{2}H_{leaf}$ values were similarly correlated with meteorological parameters. Dual-isotope analysis showed that the $\delta^{18}O_{leaf}$ and $\delta^{2}H_{leaf}$ values were closely correlated because of their similar altitudinal and seasonal responses, and so generated a well-defined isotope line relative to the local meteoric water line (LMWL). We also compared the measured $\delta^{18}O_{leaf}$ and $\delta^{2}H_{leaf}$ values with predicted values by the Craig-Gordon model, and found no significant differences between them. We demonstrate that the first-order control on $\delta^{18}O_{leaf}$ and $\delta^{2}H_{leaf}$ values was the source water, and the second-order control was the enrichment associated with biochemical and environmental factors.

Short Summary

What controls on leaf water isotopes? We answered the question from two perspectives: respective and dual isotopes. On the one hand, the $\delta^{18}O$ and $\delta^{2}H$ values of leaf water responded to isotopes of potential source water (i.e., twig water, soil water, and precipitation) and meteorological parameters (i.e., temperature, RH, and precipitation) differently; On the other hand, dual $\delta^{18}O$ and $\delta^{2}H$ values of leaf water yielded a

https://doi.org/10.5194/hess-2022-246
Preprint. Discussion started: 7 July 2022


Hydrology and Earth System Sciences
Discussions

45 significant regression line, associated with altitude and seasonality.

46

47 Keywords: Leaf water, stable isotope, controls, seasonality, altitude

48

49 1 Introduction

50 The stable isotope compositions of oxygen and hydrogen ($\delta^{18}O$ and $\delta^{2}H$, respectively)
51 are increasingly being used as powerful tracers to follow the path of water from its input
52 as precipitation, movement through the soil, and ultimately to its release as soil
53 evaporation and leaf transpiration (Penna and Meerveld, 2019). Leaf water transpiration
54 plays a key role in regulating water balance at scales ranging from catchment to global.
55 Terrestrial plants can enrich heavier isotopes (^{2}H and ^{18}O) in leaf water via evaporative
56 fractionation through the stoma (Helliker and Ehleinger, 2000; Liu et al., 2015;
57 Cernusak et al., 2016), which is highly dependent on atmospheric conditions (e.g.,
58 temperature and relative humidity) and biophysiological processes (Farquhar et al.,
59 2007; Kahmen et al., 2011; Cernusak et al., 2016). Subsequently, the isotopic signals
60 from the leaf water are integrated into plant organic matter, such as cellulose (e.g.,
61 Barbour, 2007; Lehman et al., 2017) and leaf wax (Liu et al., 2016, 2021), as powerful
62 proxies used for paleoclimate reconstruction (Pagani et al., 2006; Schefuβ et al., 2011;
63 Hepp et al., 2020). However, although leaf water isotopes are the fundamental
64 parameters in ecohydrology and organic biosynthesis, we still lack an adequate
65 understanding of what controls on leaf water isotopes, or the relative importance of
66 source water and hydroclimates controls leaf water isotopes?

https://doi.org/10.5194/hess-2022-246
Preprint. Discussion started: 7 July 2022


Hydrology and Earth System Sciences
Discussions

67

68 $\delta^{18}O_{leaf}$ and $\delta^{2}H_{leaf}$ values are influenced firstly by a plant's source water (mainly water
69 taken up by roots from the soil; Cernusak et al., 2016; Barbour et al., 2017; Munksgaard
70 et al., 2017), and secondly by the enrichment associated with transpiration (Munksgaard
71 et al., 2017). Soil water for terrestrial plants generally originates from local precipitation,
72 and precipitation isotopes vary spatially and temporally, being subject to controls
73 including temperature, altitude, latitude, distance from the coast, and amount of
74 precipitation (Bowen, 2010; Bowen and Good, 2015; Cernusak et al., 2016). More
75 specifically, soil water isotopes are determined by a mixture of individual precipitation
76 events with distinct isotopic signals and are also affected by evaporation, both of which
77 lead to the development of isotopic gradients in soil water with depth (Allison et al.,
78 1983; Liu et al., 2015). A number of studies have shown that the $\delta^{18}O$ and $\delta^{2}H$ values
79 of root/xylem water can be used to characterize the water sources used by plants
80 (Rothfuss and Javaux, 2017; Wu et al., 2018; Wang et al., 2019; Amin et al., 2020; Zhao
81 et al., 2020; Liu et al., 2021a). These studies rested substantially on the assumption that
82 no isotopic fractionation of $\delta^{18}O$ and $\delta^{2}H$ values occurs during water uptake by plant
83 roots (Dawson and Ehleringer, 1991; Ehleringer and Dawson, 1992; Chen et al., 2020),
84 except in saline or xeric environments (Lin and Sternberg, 1993; Ellsworth and
85 Williams, 2007). Some recent studies have shown, however, that the occurrence of
86 isotopic fractionation during root water uptake was probably more common than
87 previously thought, especially with respect to $\delta^{2}H$ values (Zhao et al., 2016; Wang et
88 al., 2017; Barbeta et al., 2019; Poca et al., 2019; Liu et al., 2021a).

https://doi.org/10.5194/hess-2022-246
Preprint. Discussion started: 7 July 2022

In addition to the plant source water, leaf water is also isotopically enriched through the evaporative process of transpiration. The enrichment of ^{18}O and ^{2}H by leaf water transpiration can be predicted using the Craig-Gordon model (C-G model), which was originally proposed to describe evaporative enrichment of a freely evaporating water body (Craig and Gordon, 1965) but has since been modified for plant leaves under steady-state conditions (Dongmann et al., 1974; Farquhar and Cernusak, 2005). However, the C-G model fails to explain the intra-leaf heterogeneity of $\delta^{18}O_{leaf}$ and $\delta^{2}H_{leaf}$ (Cernusak et al., 2016; Liu et al., 2021b), which is currently explained using a two-pool model (Leaney et al., 1985; Song et al., 2015) and/or an advection diffusion model, as the *Péclet* effect (Farquhar and Lloyd, 1993; Farquhar and Gan, 2003). Subsequently, more complicated models have been developed to cover non-steady-state conditions (Ogée et al., 2007). These models put the emphasis on a mechanistic understanding of leaf water isotopic fractionation, but the relevant parameters cannot be strictly constrained or precisely monitored, which hinders the use of these models under natural conditions (Plavcová et al., 2018).

In this study, we combined the effects of measured source water isotopes and C-G model-predicted transpiration on $\delta^{18}O_{leaf}$ and $\delta^{2}H_{leaf}$ values. Our objectives were to deeply understanding the controls on the $\delta^{18}O_{leaf}$ and $\delta^{2}H_{leaf}$ values, and how these controls vary with the seasons. Based upon these objectives, we repeatedly sampled soils, twigs, and leaves in May, July, and September (representing spring, summer, and

https://doi.org/10.5194/hess-2022-246
Preprint. Discussion started: 7 July 2022

111 autumn, respectively) from the same 10 plots that were distributed along an elevation
112 transect. Simultaneously, we obtained the relevant meteorological parameters (e.g.,
113 temperature, relative humidity, and precipitation) from sites close to the sampling plots
114 along the transect and used these to predict the $\delta^{18}O_{leaf}$ and $\delta^{2}H_{leaf}$ values. The combined
115 analysis of concurrent measurements of $\delta^{18}O$ and $\delta^{2}H$ values in soil water, twig water,
116 and leaf water with the predicted $\delta^{18}O$ and $\delta^{2}H$ values of leaf water from the C-G model
117 associated with the surrounding meteorological parameters will help to identify the
118 factors that control $\delta^{18}O_{leaf}$ and $\delta^{2}H_{leaf}$ values. Furthermore, we performed an isotope-
119 based line analysis of the dual $\delta^{18}O$ and $\delta^{2}H$ values of leaf water, associated with
120 altitude and seasonality. This study will improve our understanding of the
121 environmental signals preserved within the $\delta^{18}O$ and $\delta^{2}H$ values extracted from plant
122 organic biomarkers associated with leaf water.
123

124 2. Materials and Methods

125 2.1 Study area

126 The Qinling Mountains form the dividing line between northern and southern China
127 and mark the boundary between the watersheds of the Yellow and Yangtze rivers. Mt.
128 Taibai (Fig. 1; 33. 96 °N, 107.77 °E) rises to 3767 m above sea level (asl) and is the
129 peak in the Qinling Mountains; it has a warm temperate ecosystem characterized by a
130 rich diversity of flora and fauna. The mean annual temperature at the bottom of Mt.
131 Taibai is 12.9°C, and mean annual precipitation is 609.5 mm (Zhang and Liu, 2010).
132 The climate, soil, and vegetation vary significantly along our slope transect, exhibiting

https://doi.org/10.5194/hess-2022-246
Preprint. Discussion started: 7 July 2022

a remarkable vertical geo-ecological zonation (Fig. 1). The area contains a variety of climate zones: warm temperate (< 1300 m asl), temperate (1300 - 2600 m asl), cool temperate (2600 - 3350 m asl), and alpine (> 3350 m asl). The soil types vary from yellow loess soil at low elevations, spectacular rocky outcrops at middle elevations, and glacial remnants at high elevations. The vegetation along the transect consists mainly of coniferous and broadleaf forests and alpine and subalpine vegetation (Fig. 1; Liu, 2021). The dominant species range from *Quercus variabilis*, *Q. aliena*, *Betula albosinensis*, *B. utilis*, *Abies fargessi,* and *Larix chinensis* forests to *Rhododendron clementinae* and *R. concinnum* alpine (Supplementary table S1).

2.2 Sampling strategy

Plants and soils were sampled in May, July, and September 2020, and samples were collected from 10 plots (3 × 3 m) covering all of the vegetation zones along the northern slope of Mt. Taibai, extending from 608 to 3533 m asl (Fig. 1). Among the plots, six (i.e., site 2, 3, 4, 5, 8, 10; Fig. 1) were selected as being the closest to the weather stations along the elevation transect, and they were used order to obtain the *in-situ* meteorological data for analysis. For the plants, one or two deciduous and coniferous trees were chosen in each plot, and several large leaves and suberized twigs were collected for each species. The leaf samples were conducted in the context of the intact leaves on account of the likely isotopic gradients within a leaf (Helliker and Ehleringer, 2000; Liu et al., 2016). Our sampling period was between 12 and 15 pm because maximum diurnal enrichment of the leaf water isotopic composition occurs during this part of the day (Romero and Feakins, 2011; Liu et al., 2021). The twigs were

https://doi.org/10.5194/hess-2022-246
Preprint. Discussion started: 7 July 2022


Hydrology and Earth System Sciences
Discussions

collected at the same time by cutting suberized twigs, and all of the twigs were cut into the samples that were 3-4 cm long. The leaf and twig samples were immediately placed into glass vials with screw caps and sealed with polyethylene parafilm. For the soils, 3 surface soil samples (less than 10 cm deep) were collected from around the sampled plants using a small metal scoop at each plot. All sampling plots were located on slopes far from rivers and surface water bodies, which ensured that the soil water in each plot was derived exclusively from precipitation. Although the surface soil layers were collected only as being representative of soil water in this study, these samples could provide a relatively good source of water for the plants, as supported by a prior study conducted along the same elevation transect (Zhang and Liu, 2010). The soil samples were tightly sealed in a polyethylene zipper bag on site. All plant and soil samples were stored in a cool box (~ 4 °C) in the field and immediately transported to the laboratory. The altitude of each plot was determined using a handheld GPS unit with an error of ± 5 m.

2.3 Isotope analysis

The water in the plant and soil samples was extracted using an automatic cryogenic vacuum extraction system (LI-2100 Pro, LICA United Technology Limited, Beijing, China). The auto-extraction process was set for 3 hours, and the extraction rate of water from samples was more than 98%. The isotopic composition of soil water was measured using a Picarro L2130-I isotope water analyzer (Sunnyvale, CA, USA) at the State Key Laboratory of Loess and Quaternary Geology, Institute of Earth Environment, Chinese Academy of Sciences. The analytical accuracies were ±0.1‰ for $\delta^{18}O$ and ±1‰ for

https://doi.org/10.5194/hess-2022-246
Preprint. Discussion started: 7 July 2022


Hydrology and Earth System Sciences
Discussions

177 δ^2H. The isotopic measurements of twig and leaf water were conducted using an isotope
178 ratio mass spectrometer coupled to a high-temperature conversion elemental analyzer
179 (HT2000 EA-IRMS, Delta V Advantage; Thermo Fisher Scientific, Inc. USA) at the
180 Huake Precision Stable Isotope Laboratory on the campus of Tsinghua Shenzhen
181 International Graduate School. The measurement precisions were ± 0.2‰ and ± 1‰
182 for $\delta^{18}O$ and δ^2H, respectively. The isotopic composition of $\delta^{18}O$ and δ^2H is expressed
183 as an isotopic ratio:

184 $$\delta_{sample}(‰) = \left(\frac{R_{sample} - R_{standard}}{R_{standard}}\right) \times 1000 \quad (1)$$

185 where δ_{sample} represents $\delta^{18}O$ or δ^2H, and R_{sample} and $R_{standard}$ indicate the ratio
186 of $^{18}O/^{16}O$ or $^2H/^1H$ of the sample and standard, respectively. The $\delta^{18}O$ and δ^2H values
187 are reported relative to the Vienna mean standard ocean water (VSMOW). In addition,
188 the mean monthly $\delta^{18}O$ and δ^2H values of precipitation were determined using the
189 Online Isotope in Precipitation Calculator (Bowen and Revenaugh, 2003).

190 2.4 Modeling isotopes of leaf water

191 The C-G equation can be approximated as (Cernusak et al., 2022),

192 $$\delta_e = \delta_s + \varepsilon^+ + \varepsilon_k + (\delta_v - \delta_s - \varepsilon_k) \times \frac{e_a}{e_i} \quad (2)$$

193 where δ_e is the predicted $\delta^{18}O$ and δ^2H values at the evaporative sites within leaves,
194 δ_s is the $\delta^{18}O$ and δ^2H values of source water (equivalent to twig water in our study),
195 ε^+ is the equilibrium fractionation between liquid water and vapour, and ε_k is the
196 kinetic fractionation during the diffusion of vapour through the stomata and the
197 boundary layer.

198 In our analysis, we calculated Δ_v (the enrichment of atmospheric vapour relative to

https://doi.org/10.5194/hess-2022-246
Preprint. Discussion started: 7 July 2022


Hydrology and Earth System Sciences
Discussions
Open Access
EGU

source water) as $\Delta_v = (\delta_v - \delta_s)/(1+\delta_s)$, and the values of Δ_v is often close to $-\varepsilon^+$ at the isotopic steady state (Barbour, 2007; Cernusak et al., 2016); therefore we can calculate δ_v as $\delta_v = -\varepsilon^+ + (1-\varepsilon^+)\delta_s$. In addition, $\frac{e_a}{e_i}$ is the ratio of the water vapour pressure fraction in the air relative to that in the intercellular spaces and is equal to the relative humidity (RH) in the air at the steady state (Cernusak et al., 2022). Thus, Equation (2) can be derived as,

$$\delta_e = (1-h)(\varepsilon^+ + \varepsilon_k) + (1-\varepsilon^+ h)\delta_s \quad (3)$$

In Equation (3), δ_s represents the isotopic values of twig water, and h is the mean annual or monthly RH (MARH or MMRH) in this study. The equilibrium fractionation (ε^+) varies as a function of temperature (Bottinga and Craig, 1969), and can be equated to $\delta^{18}O$ and δ^2H, as follows (Majoube, 1971):

$$\varepsilon_o^+(‰) = \left[\exp\left(\frac{1.137}{(273+T)^2}\times 10^3 - \frac{0.4156}{273+T} - 2.0667\times 10^{-3}\right) - 1\right]\times 1000 \quad (4)$$

$$\varepsilon_H^+(‰) = \left[\exp\left(\frac{24.844}{(273+T)^2}\times 10^3 - \frac{76.248}{273+T} + 52.612\times 10^{-3}\right) - 1\right]\times 1000 \quad (5)$$

The kinetic fractionation (ε_k) can be calculated for $\delta^{18}O$ and δ^2H as (Farquhar et al., 2007):

$$\varepsilon_k^O(‰) = \frac{28r_s + 19r_b}{r_s + r_b} \quad (6)$$

$$\varepsilon_k^H(‰) = \frac{25r_s + 17r_b}{r_s + r_b} \quad (7)$$

where r_s and r_b are the resistances of the stomatal and boundary layers, respectively, and the inverse of the conductance of the stomatal and boundary layers, respectively. Previous studies found stomatal and boundary layer conductance values of 0.49 and 2.85 mol m^{-2} s^{-1}, respectively (Cernusak et al., 2016; Munksgaard et al., 2017), resulting in ε_k^O and ε_k^H values of 26.7 and 23.8, respectively.

https://doi.org/10.5194/hess-2022-246
Preprint. Discussion started: 7 July 2022


Hydrology and Earth System Sciences
Discussions

221 2.5 Statistical analysis

222 Statistical analysis (i.e., the mean, maximum and minimum values, as well as the
223 standard deviation) of the isotopes extracted from the precipitation, soil, twig, and leaf
224 samples was performed to define the range and distribution of the $\delta^{18}O$ and $\delta^{2}H$ values
225 across the seasons. The Pearson correlation method was used to assess the various
226 correlations between the $\delta^{18}O$ and $\delta^{2}H$ values among the different water types (i.e.,
227 precipitation, soil water, twig water, and leaf water). Hierarchical cluster analysis was
228 used to show the relationships among $\delta^{18}O_{leaf}$ and $\delta^{2}H_{leaf}$ values and potential source
229 water isotopes ($\delta^{18}O$ and $\delta^{2}H$ values in precipitation, soil water, twig water, and leaf
230 water), and meteorological parameters such as mean annual and monthly precipitation
231 (MAP and MMP), mean annual and monthly temperature (MAT and MMT), and mean
232 annual and monthly relative humidity (MARH and MMRH). A one-way analysis of
233 variance (ANOVA) combined with a *post hoc* Tukey's least significant difference (LSD)
234 test was performed to identify the significant differences in the isotopic compositions
235 of precipitation, soil, twig, and leaf waters across the months. Comparisons of the
236 relationships of $\delta^{18}O$ and $\delta^{2}H$ in the soil and leaf water were performed by using
237 analysis of covariance (ANCOVA) to compare slopes across months. The structural
238 equation model (SEM) was used to explain the respective effects of source waters (i.e.,
239 twig water, soil water, and precipitation) and meteorological parameters (i.e.,
240 temperature, precipitation, and RH) on $\delta^{18}O_{leaf}$ and $\delta^{2}H_{leaf}$ values. The validated SEMs
241 generated a good model fit, as indicated by a non-signi*fi*cant χ^2 test ($p > 0.05$), a high
242 comparative fit index (CFI > 0.95), and a low root mean square error of approximation

https://doi.org/10.5194/hess-2022-246
Preprint. Discussion started: 7 July 2022


Hydrology and Earth System Sciences
Discussions

(RMSEA < 0.05). A special SEM was constructed based on the Mantel R values in AMOS (version 24.0.0). Moreover, we used the Hybrid Single-Particle Lagrangian Integrated Trajectory (HYSPLIT) model (Draxler and Rolph, 2003) to calculate air mass back-trajectory for a central site (34.13°N, 107.83°E, 2270 m asl) in the study area. These trajectories were initiated four times daily (at 00:00, 06:00, 12:00, and 18:00 UTC) and their air parcel was released at 2300 m asl for May, July, and September 2020 and moved backwards by winds for 120 h (5 days).

3. Results

3.1 Differing response of $\delta^{18}O$ and $\delta^{2}H$ values of leaf water

The measured $\delta^{18}O$ and $\delta^{2}H$ values of leaf water responded differently to source water isotopes (Fig. 2a) and meteorological parameters (Fig. 2b) across the seasons. Cluster analysis showed that the leaf water $\delta^{18}O$ and $\delta^{2}H$ values ($\delta^{18}O_{leaf}$ and $\delta^{2}H_{leaf}$) were clustered with the twig water $\delta^{18}O$ and $\delta^{2}H$ values ($\delta^{18}O_{twig}$ and $\delta^{2}H_{twig}$; Fig. 2a), and also with MARH, MAT, and MMT (Fig. 2b). The $\delta^{2}H_{leaf}$ values were more closely correlated with isotopes of the potential source waters (e.g., twig water, soil water, and precipitation) than the $\delta^{18}O_{leaf}$ values in different months (Fig. 2a), whereas leaf water $\delta^{18}O$ and $\delta^{2}H$ values were comparatively correlated with meteorological parameters (Fig. 2b) across months. These correlations were more significant in summer (July) and autumn (September) than those in spring (May).

3.2 Comparisons of measured and predicted $\delta^{18}O$ and $\delta^{2}H$ values of leaf water

https://doi.org/10.5194/hess-2022-246
Preprint. Discussion started: 7 July 2022


Hydrology and Earth System Sciences
Discussions

The $\delta^{18}O_{leaf}$ and $\delta^{2}H_{leaf}$ values predicted by the C-G model were compared with the measured $\delta^{18}O$ and $\delta^{2}H$ values across all three months (Fig. 3). The C-G models explained 49% and 70% of the observed variations in the $\delta^{18}O_{leaf}$ and $\delta^{2}H_{leaf}$ values, respectively (Fig. 3a, c). The slopes of the relationships for both $\delta^{18}O$ and $\delta^{2}H$ values of leaf water were less than one, which suggests that part of the bulk leaf water is derived from unenriched vein water. However, there were no significant differences in $\delta^{18}O_{leaf}$ ($p = 0.54$; Fig. 3b) and $\delta^{2}H_{leaf}$ values ($p = 0.93$; Fig. 3d) between the C-G model predicted values and the measured values.

3.3 Variation of $\delta^{18}O$ and $\delta^{2}H$ values of different waters with seasons and altitude

There was a significant correlation between $\delta^{18}O_{leaf}$ and $\delta^{2}H_{leaf}$ values ($R^2 = 0.81$, $p < 0.01$; Fig. 4), with significant clusters of $\delta^{18}O_{leaf}$ and $\delta^{2}H_{leaf}$ values across the months, and values being higher in May, intermediate in July, and lower in September (Fig. 4). Within each month, the $\delta^{18}O_{leaf}$ and $\delta^{2}H_{leaf}$ values were depleted in ^{2}H and ^{18}O at higher altitudes relative to lower altitudes. Likewise, the potential types of source water (i.e., twig water, soil water, and precipitation) exhibited consistent variations across the months, showing values that were relatively higher in May, intermediate in July, and lower in September (Supplementary Fig. S1). The correlations between $\delta^{18}O$ and $\delta^{2}H$ values among the source waters were also significant (Supplementary Fig. S2), but the slopes and coefficients of determination (R^2) between the $\delta^{18}O$ and $\delta^{2}H$ values showed decreasing trends for precipitation, soil water, twig water, and leaf water from the three sampling months, except for soil water in May (Supplementary Fig. S2). In addition,

https://doi.org/10.5194/hess-2022-246
Preprint. Discussion started: 7 July 2022

the ANCOVA tests showed no significant differences for the regression lines for precipitation (df = 0.47, $F = 2.49$, $p = 0.11 > 0.05$), twig water (df = 53.2, $F = 0.42$, $p = 0.66 > 0.05$), and leaf water (df = 437.3, $F = 2.78$, $p = 0.08 > 0.05$) across the months, but a significant difference for soil water across the months (df = 308.8, $F = 10.9$, $p < 0.05$).

4. Discussion

4.1 $\delta^{18}O$ and $\delta^{2}H$ values of leaf water

A recent global meta-analysis indicated that $\delta^{18}O_{leaf}$ and $\delta^{2}H_{leaf}$ values reflect environmental drivers differently and showed that $\delta^{2}H_{leaf}$ values more strongly reflect xylem water and atmospheric vapour $\delta^{2}H$ values, whereas $\delta^{18}O_{leaf}$ values more strongly reflect air relative humidity (Cernusak et al., 2022). Our seasonal and localized observations along an elevation transect on the Chinese Loess Plateau supported these differing responses of $\delta^{18}O_{leaf}$ and $\delta^{2}H_{leaf}$ values to isotopic composition of the potential source water and meteorological parameters (Fig. 2). We found stronger correlations between $\delta^{2}H_{leaf}$ and isotope values of the source water (twig water, soil water, and precipitation) than between $\delta^{18}O_{leaf}$ values and the source water isotope values (Fig. 2a). This is consistent with the global meta-analysis (Cernusak et al., 2022). However, our localized observational study did not show a significantly different response of $\delta^{18}O_{leaf}$ and $\delta^{2}H_{leaf}$ values to meteorological parameters, and they responded at an almost equivalent magnitude (Fig. 2b). These observations suggest that plant organic isotopic proxies such as leaf wax (Sachse et al., 2012; Liu et al., 2016) and cellulose (Barbour,

https://doi.org/10.5194/hess-2022-246
Preprint. Discussion started: 7 July 2022

2007; Lehman et al., 2017), which originate from $\delta^{18}O_{leaf}$ and $\delta^{2}H_{leaf}$ values, can provide comparative information that indicates climatic signals (e.g., temperature, RH, and precipitation) in natural archives. These results argued with the recent global meta-analysis that $\delta^{18}O_{leaf}$ and $\delta^{2}H_{leaf}$ values reflect climatic parameters (i.e., RH and temperature) differently (Cernusak et al., 2022).

The results of the cluster analysis showed that the isotope values of leaf water ($\delta^{18}O_{leaf}$ and $\delta^{2}H_{leaf}$) and twig water ($\delta^{18}O_{twig}$ and $\delta^{2}H_{twig}$) were clustered into one group, but those of soil water ($\delta^{18}O_{soil}$ and $\delta^{2}H_{soil}$) and precipitation ($\delta^{18}O_{p}$ and $\delta^{2}H_{p}$) were clustered into another (Fig. 2a). This indicates that the direct source water of $\delta^{18}O_{leaf}$ and $\delta^{2}H_{leaf}$ should be $\delta^{18}O_{twig}$ and $\delta^{2}H_{twig}$, providing the source water isotope basis for the C-G model. In the C-G model (see Equation 2), besides the source water isotopes, the equilibrium fractionation factor (ε^{+}) and atmospheric vapour enrichment (Δ_v) depend on the temperature at the isotopic steady state. Thus, the $\delta^{18}O_{leaf}$ and $\delta^{2}H_{leaf}$ values were predicted to be associated primarily with temperature, RH, and source water, which is consistent with the results from the cluster analysis that the $\delta^{18}O_{leaf}$ and $\delta^{2}H_{leaf}$ values were clustered with temperature (MAT and MMT) and RH (MARH; Fig. 2b). Based on the C-G model, we plotted the measured and predicted $\delta^{18}O_{leaf}$ and $\delta^{2}H_{leaf}$ values (Fig. 3a, c) and observed no significant differences between the measured and predicted values of $\delta^{18}O_{leaf}$ and $\delta^{2}H_{leaf}$ values (Fig. 3b, d). Although the slopes of the predicted and measured $\delta^{18}O_{leaf}$ and $\delta^{2}H_{leaf}$ values were less than one, the C-G model still provides a reasonable framework for guiding analysis of the different controls on

https://doi.org/10.5194/hess-2022-246
Preprint. Discussion started: 7 July 2022

331 $\delta^{18}O_{leaf}$ and $\delta^{2}H_{leaf}$ values.

332

333 4.2 Dual $\delta^{18}O$ and $\delta^{2}H$ plots of leaf water

334 There was a significant linear correlation between the $\delta^{18}O_{leaf}$ and $\delta^{2}H_{leaf}$ values, with
335 remarkable clusters associated with the three months analyzed in this study (Fig. 4). As
336 is well-known, the LMWL, generated by precipitation $\delta^{18}O$ and $\delta^{2}H$ values at the local
337 scale, serves as an important reference line for inter-comparisons among different
338 waters. Furthermore, the regression lines of the $\delta^{18}O$ and $\delta^{2}H$ values from soil water,
339 twig water, and leaf water (Supplementary Fig. S2) suggest that the leaf water isotopes
340 could well inherit isotopic signals of source waters that originate from twig water, soil
341 water, and ultimately precipitation. The slopes and intercepts of the $\delta^{18}O$ and $\delta^{2}H$ values
342 decreased significantly from precipitation, soil water, twig water, and leaf water for
343 each month, except for soil water in May (Supplementary Fig. S2). Such patterns have
344 been observed in the a number of previous calibration studies (Brooks et al., 2010;
345 Evaristo et al., 2015; Sprenger et al., 2016, 2017; Wang et al., 2017; Benettin et al.,
346 2018; Barbeta et al., 2019; Penna and Meerveld, 2019; Liu et al., 2021a). The slopes of
347 the LMWLs were lower in July (6.79) relative to those from May (7.04) and September
348 (6.85), but were not significantly different (ANCOVA test: df = 0.47, $F = 2.49$, $p = 0.11 >$
349 0.05). This suggests that the local water vapour from precipitation was derived from the
350 same source across the seasons, but was subject to different intensities of evaporation
351 as the temperature changed through the seasons (Li et al., 2019; Wu et al., 2019, 2021).
352 The slopes of the $\delta^{18}O$ and $\delta^{2}H$ values from the soil, twig, and leaf waters were also

https://doi.org/10.5194/hess-2022-246
Preprint. Discussion started: 7 July 2022

much smaller than the LMWLs across the months due to the occurrence of secondary evaporation in the other water types.

In the dual isotope plot of leaf water, there were well-defined clusters of $\delta^{18}O_{leaf}$ and $\delta^{2}H_{leaf}$ values across the three months: ^{18}O and ^{2}H were depleted in September, there were intermediate values in July, and ^{18}O and ^{2}H were enriched in May (Fig. 4). When focusing on each month, relatively higher isotopic values occurred at low elevations, but lower isotopic values were present at high elevations despite there being no, or only weak, correlations between the the $\delta^{18}O_{leaf}$ and $\delta^{2}H_{leaf}$ values and altitude (Supplementary Fig. S3). The correlations between the $\delta^{18}O_{leaf}$ and $\delta^{2}H_{leaf}$ values and altitude, and between the $\delta^{18}O_{twig}$ and $\delta^{2}H_{twig}$ values and altitude, were not significant and weak across the three months; however, the $\delta^{18}O_{p}$ and $\delta^{2}H_{p}$, and also the $\delta^{18}O_{soil}$ and $\delta^{2}H_{soil}$ values, were significantly correlated with altitude (Supplementary Fig. S3), which suggests that besides source water (precipitation and soil water), other factors associated with plants also affect the $\delta^{18}O_{leaf}$ and $\delta^{2}H_{leaf}$ values.

The dual isotope plot of $\delta^{18}O_{leaf}$ and $\delta^{2}H_{leaf}$ values show a significant isotope line: $y = 4.52x - 50.7$ ($R^2 = 0.81$, $p < 0.01$; Fig. 4), but relatively shallower slopes (3.53, 1.86, and 2.81 in May, July, and September, respectively) of $\delta^{18}O_{leaf}$ and $\delta^{2}H_{leaf}$ values were observed across the seasons (Supplementary Fig. S2). Such a correlation was supported by a recent study that conducted consecutive measurements of $\delta^{18}O$ and $\delta^{2}H$ values in xylem/leaf water in Switzerland and indicated that leaf water provided great potential

https://doi.org/10.5194/hess-2022-246
Preprint. Discussion started: 7 July 2022

375 to determine the source water of plants (Benettin et al., 2021). Our local study showed
376 remarkable clusters in the measured (Fig. 4) and the C-G model predicted (Fig. 3)
377 $\delta^{18}O_{leaf}$ and $\delta^{2}H_{leaf}$ values across the months and the consistencies of respective $\delta^{18}O_{leaf}$
378 and $\delta^{2}H_{leaf}$ values with potential source water isotopes across months (Supplementary
379 Fig. S1). These findings of temporally consistent dynamics among the water types (i.e.,
380 precipitation, soil water, twig/stem water, and leaf water) have been observed in a
381 number of previous studies (Phillips and Ehleringer, 1995; Cernusak et al., 2005;
382 Sprenger et al., 2016; Berry et al., 2017; Liu et al., 2021a).
383
384 The isotopic inheritance from precipitation to leaf water indicate that seasonal
385 variations of $\delta^{18}O_{p}$ and $\delta^{2}H_{p}$ values are the first-order control on the temporal patterns
386 seen in the leaf water. The seasonal dynamics of the $\delta^{18}O_{p}$ and $\delta^{2}H_{p}$ values reflect the
387 combined effects of such things as temperature, altitude, and precipitation amount,
388 which are associated with orographic conditions, as well as sub-cloud evaporation,
389 moisture recycling, and differences in the vapor source (Dansgaard, 1964; McGuire and
390 McDonnell, 2007; Li et al., 2016; Penna and Meerveld, 2019; Wu et al., 2019). In this
391 study, we used the HYSPLIT model to demonstrate the ultimate cause of the seasonal
392 variations of $\delta^{18}O_{leaf}$ and $\delta^{2}H_{leaf}$ values; that is, the monthly dynamics of the $\delta^{18}O_{p}$ and
393 $\delta^{2}H_{p}$ values. The monthly variations of the $\delta^{18}O_{p}$ and $\delta^{2}H_{p}$ values from the Global
394 Network for Isotopes in Precipitation (GNIP, http://www.iaea.org/) at Xi'an station
395 (1985-1992 AD), which is ~100 km from our study transect, were enriched in ^{18}O and
396 ^{2}H in May relative to July and September (Fig. 5a, b). The cluster mean of the moisture

https://doi.org/10.5194/hess-2022-246
Preprint. Discussion started: 7 July 2022


Hydrology and Earth System Sciences
Discussions

transport routes from HYSPLIT (Draxler and Rolph, 2003) and the climatological 850 hPa wind vectors showed that the main moisture sources were from western China and central Asia in May, the China-India Peninsula and Bay of Bengal, and local moisture recycling and convection (Fig. 5c, d, e). The seasonal variations in $\delta^{18}O_p$ and $\delta^{2}H_p$ values are consistently related to the onset, advancement, and retreat of the Asian summer monsoon and associated changes in the large-scale monsoon circulation (e.g., Zhang et al., 2020, 2021). As the summer monsoon starts in mid-May, the rainfall season starts in southern China; however, our study area is controlled mainly by moisture from the westerlies (Chiang et al., 2015) with relatively higher vapour, $\delta^{18}O_p$, and $\delta^{2}H_p$ values (Fig. 5c, a, b). In July, the summer monsoon reaches its strongest phase and the rainfall belt shifts to central and northern China, where the southerly wind brings plenty of moisture from the China-India Peninsula and the Bay of Bengal with lower vapour, $\delta^{18}O_p$, and $\delta^{2}H_p$ values (Fig. 5d, a, b). When the summer monsoon withdraws in September, the study area is controlled mainly by moisture from local moisture recycling and convection (Fig. 5e). Soil water stores the June-August monsoon rainfall with its lower $\delta^{18}O$ and $\delta^{2}H$ values, resulting in even lower $\delta^{18}O_p$ and $\delta^{2}H_p$ values in September than in July (Supplementary Fig. S1), and thus resulting in significantly lower $\delta^{18}O$ and $\delta^{2}H$ values of leaf water (Fig. 4).

4.3 Framework of controls for $\delta^{18}O$ and $\delta^{2}H$ values of leaf water

To delineate the mechanisms that control the $\delta^{18}O_{leaf}$ and $\delta^{2}H_{leaf}$ values, we used the SEMs to quantify the complex interactions among $\delta^{18}O_{leaf}$ or $\delta^{2}H_{leaf}$ values, and source

https://doi.org/10.5194/hess-2022-246
Preprint. Discussion started: 7 July 2022


Hydrology and Earth System Sciences
Discussions

419 waters, and meteorological parameters (Fig. 6). The coefficients of determination (R^2)
420 were 0.48 and 0.71 for the $\delta^{18}O_{leaf}$ and $\delta^{2}H_{leaf}$ values, respectively, indicating that the
421 models explained more variance for $\delta^{2}H_{leaf}$ values than $\delta^{18}O_{leaf}$ values (Fig. 6). The
422 SEMs showed that potential source waters (i.e., twig water, soil water, and precipitation)
423 had stronger effects on $\delta^{2}H_{leaf}$ relative to $\delta^{18}O_{leaf}$ values, while the meteorological
424 parameters showed weak effects on both $\delta^{18}O_{leaf}$ and $\delta^{2}H_{leaf}$ values (a little larger for
425 $\delta^{2}H_{leaf}$ than $\delta^{18}O_{leaf}$ values). This is consistent with our above correlation analysis (Fig.
426 2). Surprisingly, MMT had significant and strong effects on $\delta^{18}O_{p}$ and $\delta^{2}H_{p}$ values,
427 suggesting that temperature plays a key role in determining $\delta^{18}O_{p}$ and $\delta^{2}H_{p}$ values, but
428 this finding is not discussed further here. Collectively, the SEMs also showed that
429 source water exerts the first-order control but affects $\delta^{18}O_{leaf}$ and $\delta^{2}H_{leaf}$ differently; the
430 meteorological parameters had a weak control on $\delta^{18}O_{leaf}$ and $\delta^{2}H_{leaf}$, with a relatively
431 stronger effect on $\delta^{2}H_{leaf}$ than $\delta^{18}O_{leaf}$ values.
432
433 A schematic representation of the controls on $\delta^{18}O_{leaf}$ and $\delta^{2}H_{leaf}$ values (respective and
434 dual) is shown in Fig. 7, and involves multiple processes associated with the
435 hydroclimatic and biochemical factors that affect $\delta^{18}O_{leaf}$ and $\delta^{2}H_{leaf}$ values. The
436 meteorological parameters (temperature, RH, and precipitation) exerted distinct effects
437 on the $\delta^{18}O$ and $\delta^{2}H$ values of the source water, and thus on the $\delta^{18}O_{leaf}$ and $\delta^{2}H_{leaf}$ values,
438 as demonstrated above by the SEM. Significant isotopic fractionation occurred mainly
439 at two key locations across the vertical soil profiles and leaf architectures from
440 precipitation to leaf water. First, an isotopic gradient across the vertical soil profile

https://doi.org/10.5194/hess-2022-246
Preprint. Discussion started: 7 July 2022

appeared because of evaporation from the surface soil layers (Ehleringer et al., 1992; Goldsmith et al., 2012; Evaristo et al., 2015). This evaporative isotopic fractionation causes an isotopic linear trajectory down soil profile (Goldsmith et al., 2012; Rothfuss and Javaux, 2017; Wu et al., 2018; Wang et al., 2019; Amin et al., 2020; Zhao et al., 2020; Liu et al., 2021a). Second, there were significant isotopic heterogeneities associated with the $\delta^{18}O_{leaf}$ (Helliker and Ehleringer, 2000; Farquhar and Gan, 2003; Gan et al., 2003; Song et al., 2015) and $\delta^{2}H_{leaf}$ values (Šantrůček et al., 2007; Liu et al., 2016; Liu et al., 2021b) within a leaf, which depends substantially on veinal structures (Liu et al., 2021b). The within-leaf heterogeneity of the $\delta^{18}O_{leaf}$ and $\delta^{2}H_{leaf}$ values can be explained using the *Péclet*-modified C-G model (Gan et al., 2003; Farquhar and Gan, 2003; Cernusak et al., 2005, 2016).

Moreover, the hydroclimatic factors (e.g., temperature, RH, precipitation, etc.) varied with altitude and seasonality, yielding an isotopic water line (LWL) in the dual-isotope plot (Fig. 4). The slope of the LWL was shallower than the LMWL, with an intersection angle θ (Fig. 7). We speculate that θ probably varies with the hydroclimatic and biochemical factors associated with evaporation, transpiration, and biochemistry, but the relationship between θ and these hydroclimatic and biochemical factors required further exploration. Overall, the LWL is controlled primarily by altitude and seasonality, as these are the main influences on the hydroclimatic and biochemical factors.

5 Conclusion

https://doi.org/10.5194/hess-2022-246
Preprint. Discussion started: 7 July 2022


Hydrology and Earth System Sciences
Discussions

Along an elevation transect on the Chinese Loess Plateau, precipitation, soil water, twig water, and leaf water were repeatedly sampled to explore the controls on $\delta^{18}O_{leaf}$ and $\delta^{2}H_{leaf}$ values associated with meteorological parameters and source water. The effects of meteorological parameters and source water on $\delta^{18}O_{leaf}$ and $\delta^{2}H_{leaf}$ values were different, and the dual $\delta^{18}O_{leaf}$ and $\delta^{2}H_{leaf}$ plot generated an isotopic line. The $\delta^{18}O_{leaf}$ and $\delta^{2}H_{leaf}$ values were controlled by the combined effects of source water and hydroclimate that varied with altitude and season.

Competing interests

The authors declare that they have no known competing financial interests or personal relationships that could have appeared to influence the work reported in this paper.

Acknowledgement

We thank X. Cao and M. Xing for help with laboratory assistance, and Y. Cheng for the help in the field. We thank Profs. J. J. McDonnell and L. A. Cernusak for discussing and editing the paper. This work was supported by the Chinese Academy of Sciences (XDB40000000; XAB2019B02; ZDBS-LY-DQC033; 132B61KYSB20170005) and National Natural Science Foundation of China (42073017).

Author contribution

J.L. conceived the idea of research, and performed the data analysis. J.L., H.W., and H.Z. wrote the manuscript. L.G. and Y.Z. edited the paper. J.L. and C.J. performed the

https://doi.org/10.5194/hess-2022-246
Preprint. Discussion started: 7 July 2022

485 lab work. All authors contributed to discuss the results.

486

487 **Data availability statement**

488 Data related to this article can be found in Electric Annex and Mendeley Data
489 (https://data.mendeley.com/drafts/t44wybgpr3).

490

491 **References**

492 Amin, A., Zuecco, G., Geris, J., Schwendenmann, L., McDonnell, J.J., Borga, M., and
493 Penna, D.: Depth distribution of soil water sourced by plants at the global scale: a new
494 direct inference approach, Ecohydrology, 13, e2177, 2020.

495 Allison, G., Barnes, C., and Hughes, M.: The distribution of deuterium and ^{18}O in dry
496 soils 2. Experimental, J. Hydrol., 64, 377–397, 1983.

497 Barbeta, A., Jones, S. P., Clavé, L., Gimeno, T. E., Fréjaville, B., Wohl, S., and Ogée,
498 J.: Unexplained hydrogen isotope offsets complicate the identification and
499 quantification of tree water sources in a riparian forest, Hydrol. Earth Syst. Sci., 23,
500 2129–2146, 2019.

501 Barbour, M. M.: Stable oxygen isotope composition of plant tissue: a review. Funct.
502 Plant Biol., 34, 83–94, 2007.

503 Barbour, M. M., Farquhar, G. D., and Buckley, T. N.: Leaf water stable isotopes and
504 water transport outside the xylem, Plant Cell Environ., 40, 914–920, 2017.

505 Benettin, P., Nehemy, M. F., Cernusak, L. A., Kahmen, A., and McDonnell, J. J.: On
506 the use of leaf water to determine plant water source: A proof of concept, Hydrol.

https://doi.org/10.5194/hess-2022-246
Preprint. Discussion started: 7 July 2022

507 Process., DOI: 10.1002/hyp.14073, 2021.

508 Benettin, P., Volkmann, T. H. M., von Freyberg, J., Frentress, J., Penna, D., Dawson, T.
509 E., and Kirchner, J. W.: Effects of climatic seasonality on the isotopic composition of
510 evaporating soil waters, Hydrol. Earth Syst. Sci., 22, 2881–2890, 2018.

511 Berry, Z. C., Evaristo, J., Moore, G., Poca, M., Steppe, K., Verrot, L., Asbjornsen, H.,
512 Borma, L. S., Bretfeld, M., Herve-Fernandez, P., Seyfried, M., Schwendenmann, L.,
513 Sinacore, K., Wispelaere, L. D., and McDonnell, J.: The two water worlds hypothesis:
514 addressing multiple working hypotheses and proposing a way forward, Ecohydrology,
515 e1843, 2017.

516 Bottinga, Y., and Craig., H.: Oxygen isotope fractionation between CO_2 and water, and
517 the isotopic composition of marine atmospheric CO_2, Earth Planet. Sci. Lett., 5, 285–
518 295, 1969.

519 Bowen, G. J., and Revenaugh, J.: Interpolating the isotopic composition of modern
520 meteoric precipitation, Water Resour. Res., 39, 1299, 2003.

521 Bowen, G. J.: Isoscapes: Spatial pattern in isotopic biogeochemistry, Annu. Rev. Earth
522 Planet. Sci., 2010, 161–187, 2010.

523 Bowen, G. J., and Good, S. P.: Incorporating water isoscapes in hydrological and water
524 resource investigations, Wiley Interdiscip. Rev. Water, 2, 107–119, 2015.

525 Brooks, J. R., Barnard, H. R., Coulombe, R., and McDonnell, J. J.: Ecohydrologic
526 separation of water between trees and streams in a Mediterranean climate, Nat. Geosci.,
527 3, 100–104. 2010.

528 Cernusak, L. A., Farquhar, G. D., and Pate, J. S.: Environmental and physiological

https://doi.org/10.5194/hess-2022-246
Preprint. Discussion started: 7 July 2022

529 controls over oxygen and carbon isotope composition of Tasmanian blue gum,
530 *Eucalyptus globulus*, Tree Physiol., 25, 129–146, 2005.
531 Cernusak, L. A., Barbour, M. M., Arndt, S. K., Cheesman, A. W., English, N. B., field,
532 T. S., Helliker, B. R., Holloway-Phillips, M. M., Holtum, J. A. M., Kahmen, A.,
533 McInerney, F. A., Munksgaard, N. C., Simonin, K. A., Song, X., Stuart-Williams, H.,
534 West, J. B., and Farquhar, G. D.: Stable isotopes in leaf water of terrestrial plants. Plant
535 Cell Environ., 39, 1087–1102, 2016.
536 Cernusak, L. A., Barbeta, A., Bush, R., Eichstaedt R., Ferrio, J., Flanagan, L., Gessler,
537 A., Martín-Gómez, P., Hirl, R., Kahmen, A., Keitel., C., Lai, C., Munksgaard, N.,
538 Nelson, D., Ogée J., Roden, J., Schnyder, H., Voelker, S., Wang L., Stuart-Williams, H.,
539 Wingate, L., Yu, W., Zhao, L., Cuntz, M., 2022. Do ^{2}H and ^{18}O in leaf water reflect
540 environmental drivers differently? New Phytologist, DOI: 10.1111/nph.18113.
541 Chen. Y., Helliker, B. R., Tang, X., Li, F., Zhou, Y., and Song, X.: Stem water cryogenic
542 extraction biases estimation in deuterium isotope composition of plant source water,
543 Proc. Natl. Acad. Sci., 117, 33345–33350, 2020.
544 Chiang, J. C., Fung, I. Y., Wu, C. -H., Cai, Y., Edman, J. P., Liu, Y., Day, J. A.,
545 Bhattacharya, T., Mondal, Y., and Labrousse, C. A.: Role of seasonal transitions and
546 westerly jets in East Asian paleoclimate, Quat. Sci. Rev., 108, 111–129, 2015.
547 Craig, H., and Gordon, L. I.: Deuterium and oxygen-18 variations in the ocean and the
548 marine atmosphere. In 'Proceedings of a conference on stable isotopes in
549 oceanographic studies and paleotemperatures', pp. 9–130, 1965.
550 Dansgaard, W.: Stable isotopes in precipitation, Tellus, 16, 436–468, 1964.

https://doi.org/10.5194/hess-2022-246
Preprint. Discussion started: 7 July 2022

551 Dawson, T. E. and Ehleringer, J. R.: Streamside trees that do not use stream water,
552 Nature, 350, 335–337, 1991.
553 Dongmann. G., Nurnberg, H. E., Forstel, H., and Wagener, K.: On the enrichment of
554 $H_2{}^{18}O$ in the leaves of transpiring plants, Radiat. Environ. Biophys. 11, 41–52, 1974.
555 Draxler, R. R., and Rolph, G. D.: HYSPLIT (Hybrid Single-Particle Lagrangian
556 Integrated Trajectory) Model Access via NOAA ARLREADY. htmlNOAA Air
557 Resources Laboratory, http://www.arl.noaa.gov/ready/hysplit4, 2003.
558 Ehleringer, J. R. and Dawson, T. E: Water uptake by plants: perspectives from stable
559 isotope composition, Plant Cell Environ., 15, 1073–1082, 1992.
560 Ehleringer, J. R. and Dawson, T. E.: Water uptake by plants: perspectives from stable
561 isotope composition, Plant Cell Environ., 15, 1073–1082, 1992.
562 Ellsworth, P. Z., and Williams, D. G.: Hydrogen isotope fractionation during water
563 uptake by woody xerophytes, Plant Soil, 291, 93–107, 2007.
564 Evaristo J., Jasechko S., and McDonnell J. J.: Global separation of plant transpiration
565 from groundwater and streamflow, Nature, 525, 91–94, 2015.
566 Farquhar, G. D., Cernusak, L. A., and Barnes, B.: Heavy water fractionation during
567 transpiration, Plant Physiol., 143, 11–18, 2007.
568 Farquhar, G. D., and Cernusak, L. A.: On the isotopic composition of leaf water in the
569 non- steady state, Funct. Plant Biol., 32, 293–303, 2005.
570 Farquhar, G..D., and Gan, K..S.: On the progressive enrichment of the oxygen isotopic
571 composition of water along leaves, Plant Cell Environ., 26, 801–819, 2003.
572 Farquhar, G. D., and Lloyd, J.: Carbon and oxygen isotope effects in the exchange of

https://doi.org/10.5194/hess-2022-246
Preprint. Discussion started: 7 July 2022

573 carbon dioxide between terrestrial plants and the atmosphere. In Stable Isotopes and
574 Plant Carbon–Water Relations (eds J.R. Ehleringer, A.E. Hall, & G.D. Farquhar), pp.
575 47–70. Academic Press, San Diego, 1993.
576 Gan, K.S., Wong, S.C., Yong, J.W.H., Farquhar, G.D., 2003. Evaluation of models of
577 leaf water^{18}O enrichments of spatial patterns of vein xylem, leaf water and dry matter
578 in maize leaves. Plant Cell Environ. 26, 1479–1495.
579 Goldsmith, G. R., Munoz-Villers, L. E., Holwerda, F., McDonnell, J. J., Asbjornsen, H.,
580 and Dawson, T. E.: Stable isotopes reveal linkages among ecohydrological processes in
581 a seasonally dry tropical montane cloud forest, Ecohydrology, 5, 779–790, 2012.
582 Helliker, B. R., and Ehleringer, J. R.: Establishing a grassland signature in veins: ^{18}O in
583 the leaf water of C_3 and C_4 grasses, Proc. Natl. Acad. Sci., 97, 7894–7898, 2000.
584 Hepp, J., Schäfer, I. K., Lanny, V., Franke, J., Blidtner, M., Rozanski, K., Glaser, B.,
585 Zech, M., Eglinton, T. I., and Zech, R.: Evaluation of bacterial glycerol dialkyl glycerol
586 tetraether and ^{2}H-^{18}O biomarker proxies along a central European topsoil transect,
587 Biogeosciences, 17, 741–756, 2020.
588 Kahmen, A., Sachse, D., Arndt, S. K., Tu, K. P., Farrington, H., Vitousek, P. M., and
589 Dawson, T. E.: Cellulose δ^{18}O is an index of leaf-to-air vapor pressure difference (VPD)
590 in tropical plants, Proc. Natl. Acad. Sci., 108, 1981–1986, 2011.
591 Leaney, F., Osmond, C., Allison, G., and Ziegler, H.: Hydrogen-isotope composition of
592 leaf water in C_3 and C_4 plants: its relationship to the hydrogen-isotope composition of
593 dry matter, Planta, 164, 215–220, 1985.
594 Lehmann, M. M., Gamarra, B., Kahmen, A., Siegwolf, R. T. W., and Saurer, M.:

https://doi.org/10.5194/hess-2022-246
Preprint. Discussion started: 7 July 2022

595 Oxygen isotope fractionations across individual leaf carbohydrates in grass and tree
596 species. Plant Cell Environ., 40, 1658–1670, 2017.
597 Li, Z., Feng, Q., Wang, Q., Kong, Y., Cheng, A., Yong, S., Li, Y., Li, J., and Guo, X.:
598 Contributions of local terrestrial evaporation and transpiration to precipitation using
599 $\delta^{18}O$ and D-excess as a proxy in Shiyang inland river basin in China, Global Planet.
600 Change, 146, 140–151, 2016.
601 Li, Z., Li, Z., Yu, H., Song, L., and Ma, J.: Environmental significance and zonal
602 characteristics of stable isotope of atmospheric precipitation in arid Central Asia. Atmos.
603 Res., 227, 24–40, 2019.
604 Lin, G. H., and Sternberg, L. S. L.: Hydrogen isotopic fractionation by plant roots
605 during water uptake in coastal wetland plants. Stable Isotopic and Plant Carbon/Water
606 Relations, Academic Press, New York, pp. 497–510, 1993.
607 Liu, J., Liu, W., and An, Z.: Insight into the reasons of leaf wax $\delta D_{n\text{-alkane}}$ values between
608 grasses and woods, Sci. Bull., 60, 549–555, 2015.
609 Liu, J., Liu, W., An, Z., and Yang, H.: Different hydrogen isotope fractionations during
610 lipid formation in higher plants: Implications for paleohydrology, Sci. Report, 6, 19711,
611 2016.
612 Liu, J., Wu, H., Cheng, Y., Jin, Z., and Hu, J.: Stable isotope analysis of soil and plant
613 water in a pair of natural grassland and understory of planted forestland on the Chinese
614 Loess Plateau, Agr. Water Manage., 249, 106800, 2021a.
615 Liu, J., An, Z., and Lin, G.: Intra-leaf heterogeneities of hydrogen isotope compositions
616 in leaf water and leaf wax of monocots and dicots, Sci. Total Environ., 770, 145258,

https://doi.org/10.5194/hess-2022-246
Preprint. Discussion started: 7 July 2022

2021b.

Liu, J.: Seasonality of the altitude effect on leaf wax n-alkane distributions, hydrogen and carbon isotopes along an arid transect in the Qinling Mountains. Sci. Total Environ., 778, 146272, 2021.

Majoube M. Fractionnement en oxygen-18 et en deuterium entre l'eau et sa vapeur. Journal de Chimie et Physique 68, 1423–1436, 1971.

McGuire, K., and McDonnell J. J.: Stable isotope tracers in watershed hydrology, in Stable Isotopes in Ecology and Environmental Science, Ecological Methods and Concepts Series, pp. 334–374, 2007.

Munksgaard, N. C., Cheesman, A. W., English, N. B., Zwart, C., Kahmen, A., and Cernusak, L. A.: Identifying drivers of leaf water and cellulose stable isotope enrichment in Eucalyptus in northern Australia, Oecologia, 183, 31–43, 2017.

Ogée, J., Cuntz, M., Peylin, P., Bariac, T., 2007. Non-steady-state, non-uniform transpiration rate and leaf anatomy effects on the progressive stable isotope enrichment of leaf water along monocot leaves. Plant Cell Environ. 30, 367–387.

Pagani, M., Pedentchouk, N., Huber, M., Sluijs, A., Schouten, S., Brinkhuis, H., Damsté, J. S. S., and Dichens, G. R.: Arctic hydrology during global warming at the Palaeocene/Eocene thermal maximum, Nature, 442, 671–675, 2006.

Penna, D., and van Meerveld, H. J.: Spatial variability in the isotopic composition of water in small catchments and its effect on hydrograph separation, WIREs Water, e1367, 2019.

Phillips, S. L., and Ehleringer, J. R.: Limited uptake of summer precipitation by big

https://doi.org/10.5194/hess-2022-246
Preprint. Discussion started: 7 July 2022

639 tooth maple (*Acer grandidentatum* Nutt) and Gambels oak (*Quercus gambelii* Nutt),
640 Trees, 9, 214–219, 1995.
641 Plavcová, L., Hronková, M., Šimková, M., Květoň, J., Vráblová, M., Kubásek, J.,
642 Šantrůček, J.: Seasonal variation of $\delta^{18}O$ and $\delta^{2}H$ in leaf water of *Fagus sylvatica* L.
643 and related water compartments, J. Plant Physiol., 227, 56–65, 2018.
644 Poca, M., Coomans, O., Urcelay, C., Zeballos, S. R., Bodé, S., and Boecks, P.: Isotope
645 fractionation during root water uptake by *Acacia caven* is enhanced by arbuscular
646 mycorrhizas, Plant Soil, 441, 485–497, 2019.
647 Romero, I.C., Feakins, S.I., 2011. Spatial gradients in plant leaf wax D/H across a
648 coastal salt marsh in southern California. Org. Geochem. 42, 618–629.
649 Rothfuss, Y., and Javaux, M.: Reviews and syntheses: isotopic approaches to quantify
650 root water uptake: a review and comparison of methods, Biogeosciences, 14, 2199–
651 2224, 2017.
652 Sachse, D., Billault, I., Bowen, G.J., Chikaraishi, Y., Dawson, T.E., Feakins, S.J.,
653 Freeman, K.H., Magill, C.R., McInerney, F.A., van der Meer, M.T.J., Polissar, P.J.,
654 Robins, R.J., Sachs, J.P., Schmidt, H.L., Sessions, A.L., White, J.W.C., West, J.B.,
655 Kahmen, A., 2012. Molecular paleoyhydrology: interpreting the hydrogen-isotopic
656 composition of lipid biomarkers from photosynthesizing organisms. Annu. Rev. Earth
657 Planet. Sci. 40, 221–249.
658 Šantrůček, J., Květoň, J., Šetlík, J., Bulíčková, L., 2007. Spatial variation of deuterium
659 enrichment in bulk water of snowgun leaves. Plant Physiol. 143, 88–97.
660 Song, X., Loucos, K. E., Simonin, K. A., Farquhar, G. D., and Barbour, M. M.:

https://doi.org/10.5194/hess-2022-246
Preprint. Discussion started: 7 July 2022

661 Measurements of transpiration isotopologues and leaf water to assess enrichment
662 models in cotton, New Phytol., 206, 637–646, 2015.
663 Schefuβ, E., Kuhlmann, H., Mollenhauer, G., Prange, M., and Pätzold, J.: Forcing of
664 wet phases in Southeast Africa over the past 17,000 year, Nature, 480, 22–29, 2011.
665 Sprenger, M., Leistert, H., Gimbel, K., and Weiler, M.: Illuminating hydrological
666 processes at the soil-vegetation-atmosphere interface with water stable isotopes, Rev.
667 Geophys., 54, 674–704, 2016.
668 Sprenger, M., Tetzlaff, D., and Soulsby, S.: Soil water stable isotopes reveal evaporation
669 dynamics at the soil-plant-atmosphere interface of the critical zone, Hydrol. Earth Syst.
670 Sci., 21, 3839–3858, 2017.
671 Wang, J., Fu, B., Lu, N., and Zhang, L.: Seasonal variation in water uptake patterns of
672 three plant species based on stable isotopes in the semi-arid Loess Plateau, Sci. Total
673 Environ., 609, 27–37, 2017.
674 Wang, J., Lu, N., and Fu, B.: Inter-comparison of stable isotope mixing models for
675 determining plant water source partitioning, Sci. Total Environ. 666, 685–693, 2019b.
676 Wu, H., Li, J., Li, X., He, B., Liu, J., Jiang, Z., and Zhang, C.: Contrasting response of
677 coexisting plant's water-use patterns to experimental precipitation manipulation in an
678 alpine grassland community of Qinghai Lake watershed, China, PLoS One, 13,
679 e0194242, 2018.
680 Wu, H., Wu, J., Sakiev, K., Liu, J., Li, J., He, B., Liu, Y., and Shen, B.: Spatial and
681 temporal variability of stable isotopes ($\delta^{18}O$ and $\delta^{2}H$) in surface waters of arid,
682 mountainous Central Asia, Hydrol. Process. 33, 1658–1669, 2019.

https://doi.org/10.5194/hess-2022-246
Preprint. Discussion started: 7 July 2022

683 Wu, H., Huang, Q., Fu, C., Song, F., Liu, J., Li, J.: Stable isotope signatures of river
684 and lake water from Poyang Lake, China: Implications for river-lake interactions. J.
685 Hydrol. 592, 125619, 2021.
686 Zhang, P., and Liu, W.: Effect of plant life form on relationship between δD values of
687 leaf wax *n*-alkanes and altitude along Mount Taibai, China, Org. Geochem., 42, 100–
688 107, 2010.
689 Zhao, L., Wang, L., Cernusak, L. A., Liu, X., Xiao, H., Zhou, M., and Zhang, S.:
690 Significant difference in hydrogen isotope composition between xylem and tissue water
691 in *Populus Euphratica*, Plant Cell Environ., 39, 1848–1857, 2016.
692 Zhao, Y., Wang, Y., He, M., Tong, Y., Zhou, J., Guo, X., Liu, J., Zhang, X.: Transference
693 of *Robinia pseudoacacia* water-use patterns from deep to shallow soil layers during the
694 transition period between the dry and rainy seasons in a waterlimited region, For. Ecol.
695 Manag., 457, 117727, 2020.
696 Zhang, H., Cheng, H., Cai, Y., Spötl, C., Sinha, A., Kathayat, G., Li, H.: Effect of
697 precipitation seasonality on annual oxygen isotopic composition in the area of spring
698 persistent rain in southeastern China and its paleoclimatic implication, Clim. Past, 16,
699 211–225, 2020.
700 Zhang, H., Zhang, X., Cai, Y., Sinha, A., Spötl, C., Baker, J., Kathayat, G., Liu, Z., Tian,
701 Y., and Lu, J.: A data-model comparison pinpoints Holocene spatiotemporal pattern of
702 East Asian summer monsoon, Quat. Sci. Rev., 261, 106911, 2021.
703
704

https://doi.org/10.5194/hess-2022-246
Preprint. Discussion started: 7 July 2022


Hydrology and Earth System Sciences
Discussions
Open Access
EGU

Figure captions

Fig. 1 Sample sites (red dots) and weather stations (open triangles) that distribute along vertical vegetation zones across the Mt. Taibai transect on the Chinese Loess Plateau (a). The meteorological parameters (precipitation, temperature, and RH) vary with stations along elevation transect (b). Mean annul (MAP, MAT, MARH) and montly (MMP, MMT, MMRH) precipitation, temperature, and relative humidity. The subscripts refer to the month. The vertical vegetation distribution was adopted from Liu, 2021.

Fig. 2 Heatmaps of correlations (r) between leaf water $\delta^{18}O$ and $\delta^{2}H$ values and potential source water $\delta^{18}O$ and $\delta^{2}H$ values (twig water, soil water, and precipitation $\delta^{18}O$ and $\delta^{2}H$ values; a), and meteorological parameters (e.g., MAP, MMP, MAT, MMT, MARH, MMRH). The hierarchical cluster analysis of the isotopes of leaf water and source water (a), and meteorologica parameters (b). The subscripts (p, soil, twig, leaf) refer to precipitation, soil water, twig water, and leaf water. * Corrected significance at $p < 0.05$; ** corrected significance at $p < 0.01$; *** corrected significance at $p < 0.001$.

Fig. 3 Measured leaf water isotopic composition for $\delta^{18}O$ (a) and $\delta^{2}H$ (c) values against values predicted by the C-G model. Boxplots show no significant differences for $\delta^{18}O$ (b) and $\delta^{2}H$ (d) values between measured and predicted leaf water. The dotted lines show one-to-one lines.

Fig. 4 Correlation of leaf water $\delta^{18}O$ and $\delta^{2}H$ values across months and altitude. Leaf water $\delta^{18}O$ and $\delta^{2}H$ values were the higher in May, intermediate in July, and lower in September, and while within each month, those isotopic values were relatively lower at high altitudes and higher in lower altitudes.

Fig. 5 Variation of monthly mean precipitation $\delta^{18}O$ (a) and $\delta^{2}H$ (b) values at Xi'an station from Global Network of Isotopes in Precipitation (GNIP) and cluster mean of moisture transport routes using HYSPLIT model in May (c), July (d) and September (e), 2020. Background in (c-e) is the average precipitation (mm/day) and 850 hPa wind vectors (arrows, m/s) in May (c), July (d) and September (e) in 1979-2016 AD based on the database of the Global Precipitation Climatology Center (GPCC) (Becker et al.,

https://doi.org/10.5194/hess-2022-246
Preprint. Discussion started: 7 July 2022


Hydrology and Earth System Sciences
Discussions

2011) and the Modern-Era Retrospective analysis for Research and Applications (Rienecker et al., 2011).

Fig. 6 Structural equation model (SEM) of leaf water $\delta^{18}O$ (a) and $\delta^{2}H$ (b) values. The structural equation models considered all plausible pathways. Solid lines indicate significant positive (red) or negative (blue) effects, and dashed lines indicate non-significant effects. Grey lines indicate correlations between two variables. Numbers on the arrow indicate significant standardized path coefficients, proportional to the arrow width. The coefficients of determination (R^2) represent the proportion of variance explained by the model.

Fig. 7 Schematics of the respective and dual isotopes of $\delta^{18}O$ and $\delta^{2}H$ values from precipitation to leaf water, associated with physical (evaporation at soil profile and transpiration at leaf level) and biochemical processes. The dual isotopes of $\delta^{18}O$ and $\delta^{2}H$ values yield an isotopic water line, the slope of which was lower than the LMWL. The intersected angle varied with hydroclimates, associated with altitude and seasonality.

https://doi.org/10.5194/hess-2022-246
Preprint. Discussion started: 7 July 2022

Hydrology and Earth System Sciences
Discussions
Open Access
EGU

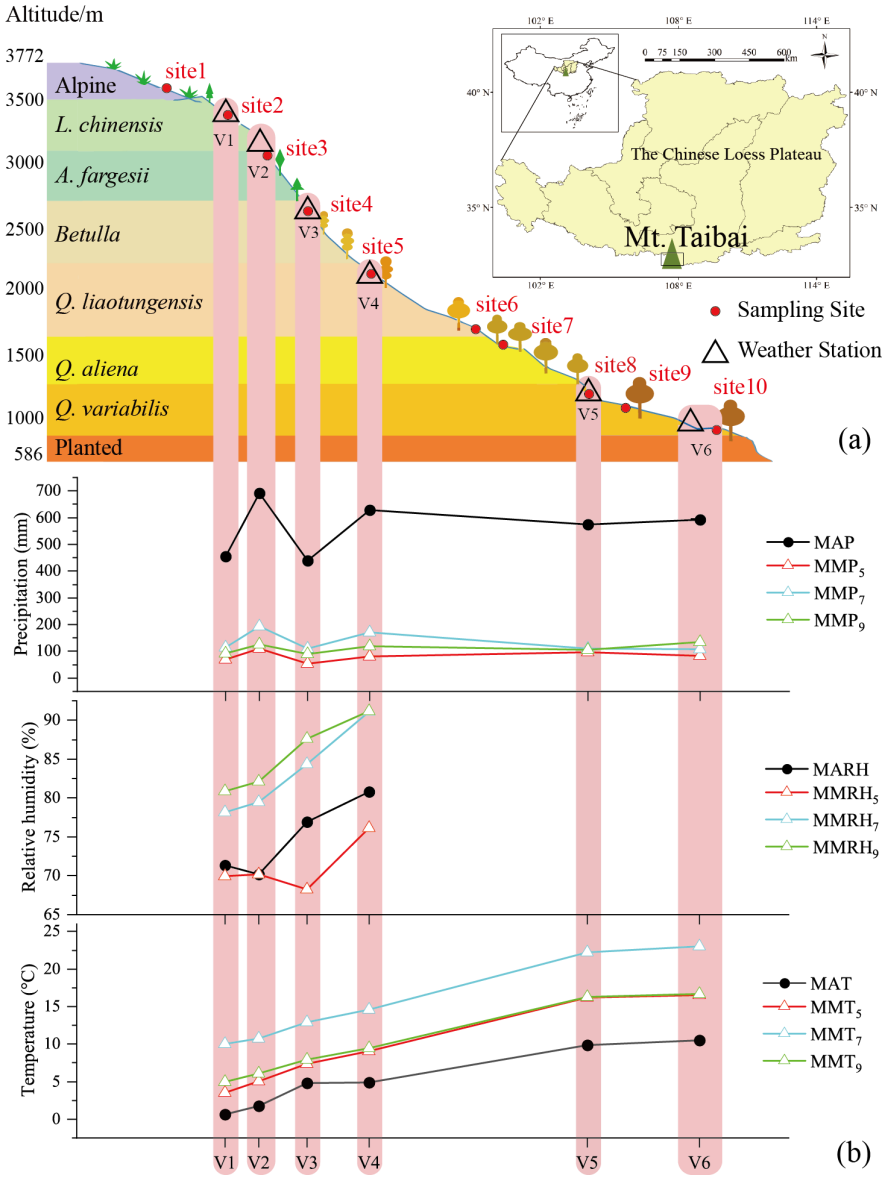

763

764 Figure-1

765

766

767

768

https://doi.org/10.5194/hess-2022-246
Preprint. Discussion started: 7 July 2022

Hydrology and Earth System Sciences
Discussions
Open Access
EGU

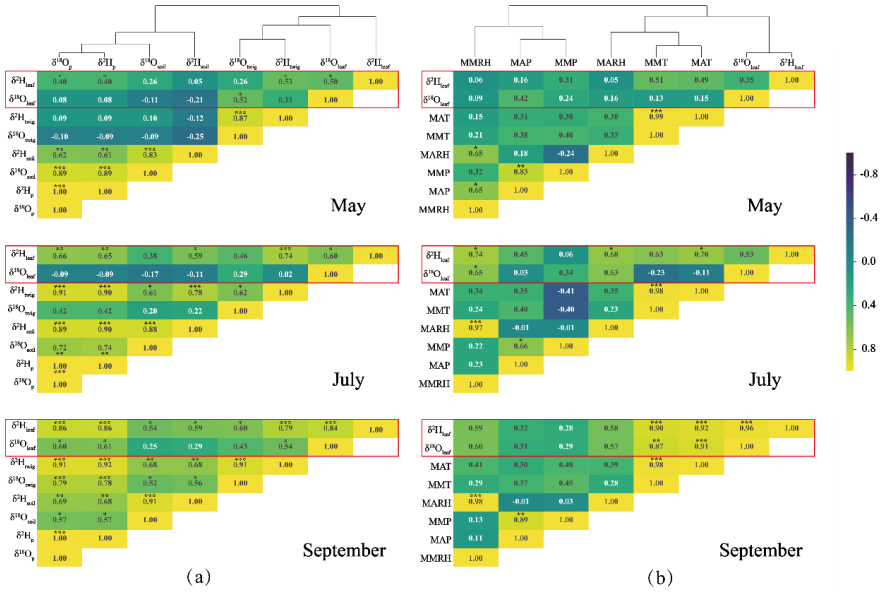

Figure-2

https://doi.org/10.5194/hess-2022-246
Preprint. Discussion started: 7 July 2022

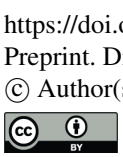

Hydrology and Earth System Sciences
Discussions
Open Access
EGU

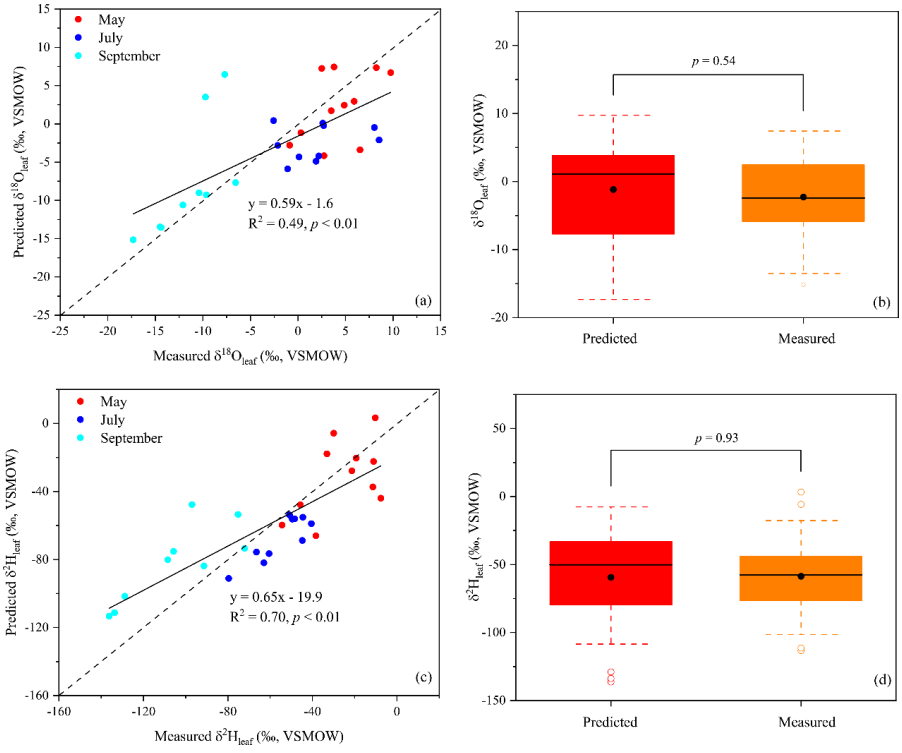

787

788 Figure-3

789

https://doi.org/10.5194/hess-2022-246
Preprint. Discussion started: 7 July 2022

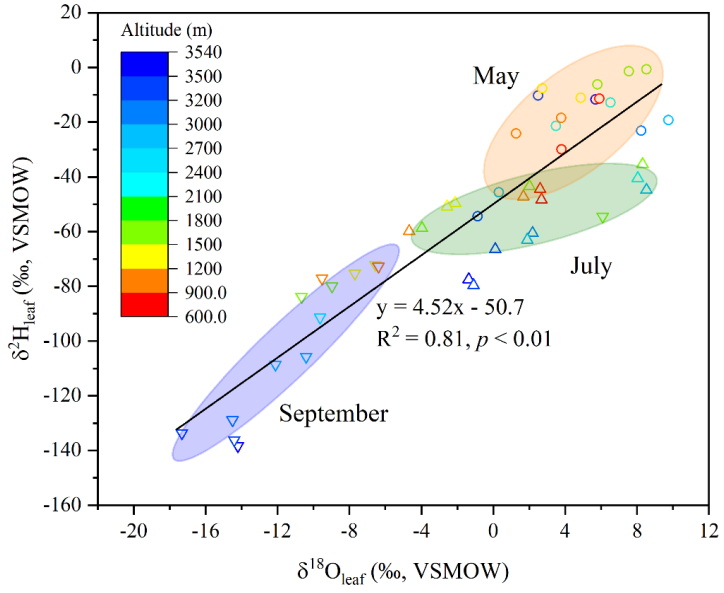

Figure-4

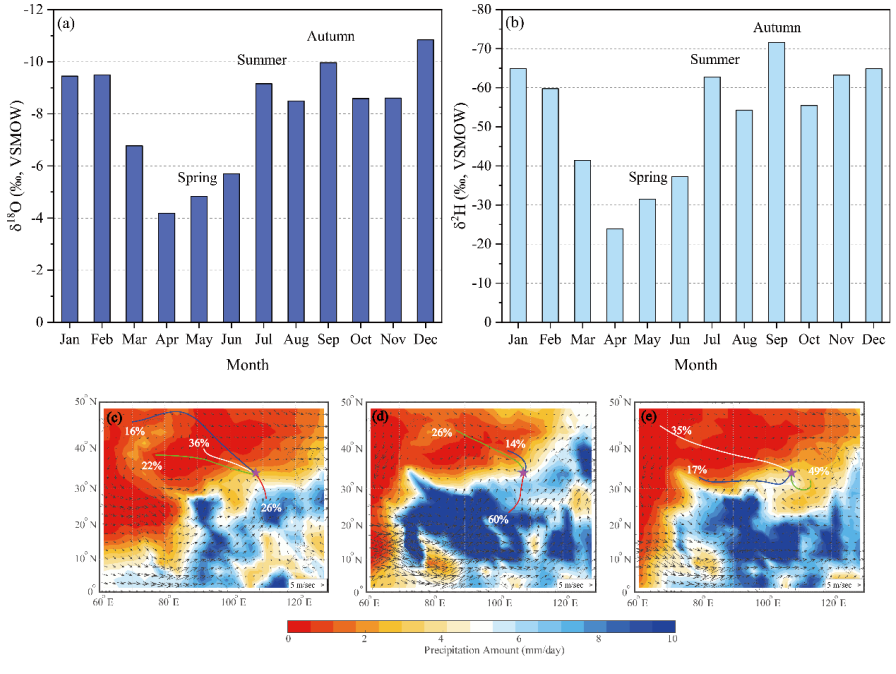

Figure-5

https://doi.org/10.5194/hess-2022-246
Preprint. Discussion started: 7 July 2022

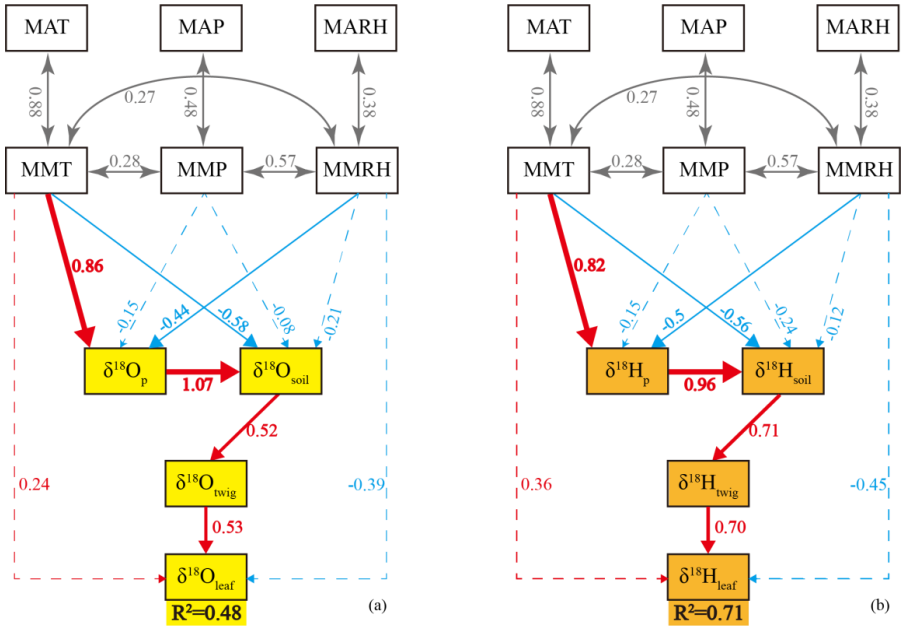

795

796 Figure-6

797

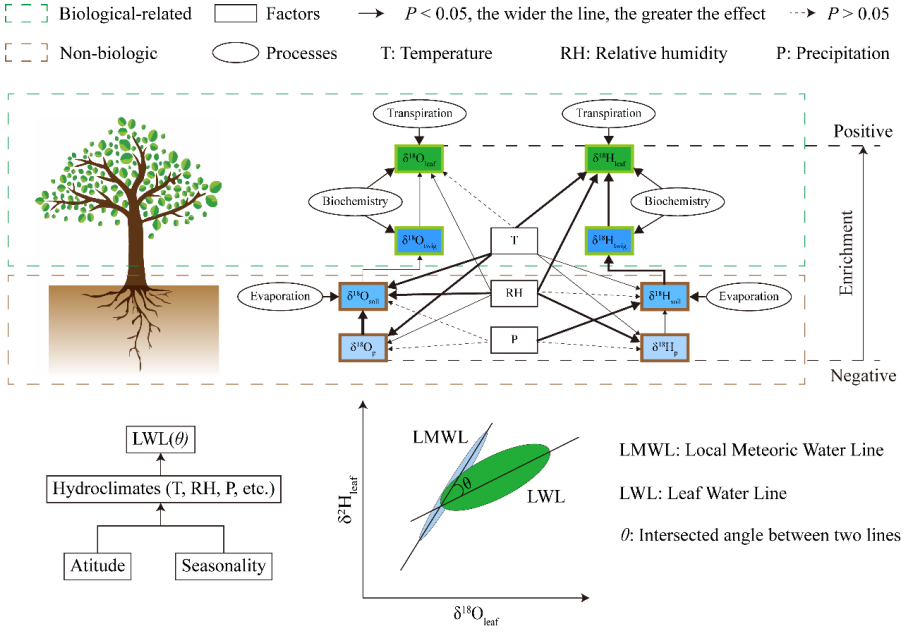

798

799 Figure-7